

PAPER • OPEN ACCESS

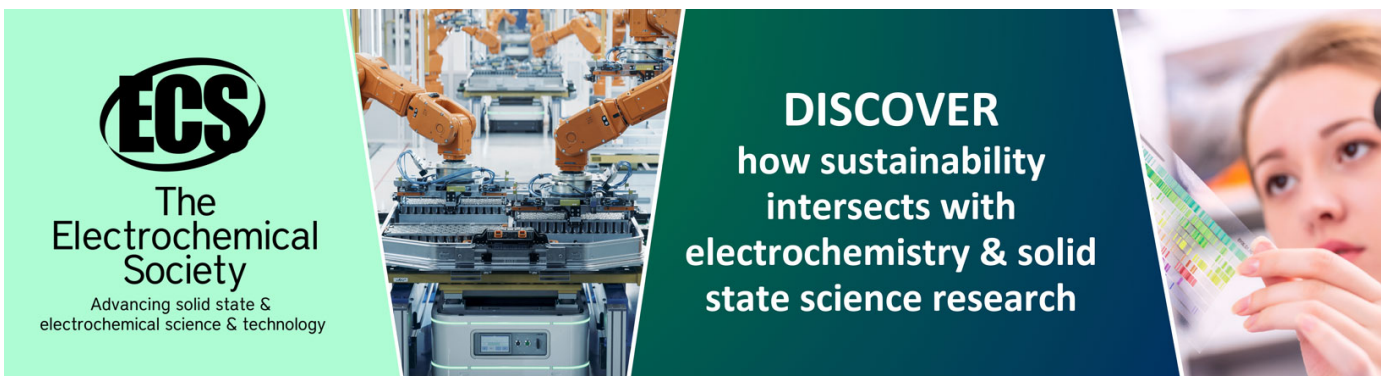
About accuracy of the discrimination parameter estimation for the dual high-energy method

To cite this article: S P Osipov *et al* 2015 *IOP Conf. Ser.: Mater. Sci. Eng.* **81** 012082

View the [article online](#) for updates and enhancements.

You may also like

- [Optimization of pulse shape discrimination based on frequency domain for SiPM-based NaI\(L\) scintillator detector](#)
JunYu Li, Peng Fan, ChengLin Zhu *et al.*
- [Adequacy Criteria of Models of the Cargo Inspection System with Material Discrimination Option](#)
S Osipov, S Chakhlov, O Osipov *et al.*
- [Contra-lateral desynchronized alpha oscillations linearly correlate with discrimination performance of tactile acuity](#)
Shiyong Su, Guohong Chai, Xinjun Sheng *et al.*



ECS
The
Electrochemical
Society
Advancing solid state &
electrochemical science & technology

DISCOVER
how sustainability
intersects with
electrochemistry & solid
state science research

About accuracy of the discrimination parameter estimation for the dual high-energy method

S P Osipov, S V Chakhlov, O S Osipov, A M Shtein, D V Strugovtsev

National Research Tomsk Polytechnic University, Lenin Avenue, 30, Tomsk, 634050, Russia

E-mail: osip1809@rambler.ru

Abstract. A set of the mathematical formulas to estimate the accuracy of discrimination parameters for two implementations of the dual high energy method – by the effective atomic number and by the level lines is given. The hardware parameters which influenced on the accuracy of the discrimination parameters are stated. The recommendations to form the structure of the high energy X-ray radiation impulses are formulated. To prove the applicability of the proposed procedure there were calculated the statistical errors of the discrimination parameters for the cargo inspection system of the Tomsk polytechnic university on base of the portable betatron MIB-9. The comparison of the experimental estimations and the theoretical ones of the discrimination parameter errors was carried out. It proved the practical applicability of the algorithm to estimate the discrimination parameter errors for the dual high energy method.

1. Introduction

The different implementations of digital radiography are widely used for the custom examination and for the flaw detection [1–4]. One of the major implementation of the digital radiography is a dual energy method (DEM) [5–8], which can discriminate the testing object (TO) materials. The discrimination for the custom examination means the correlation of test object material or their constituent with one of the extensive material classes. The mentioned division of the materials to classes is carried out by two main methods [8–11] – by effective atomic number and by level line method. In any modification of DEM on the initial stage there are generated two digital radiographs for two specially selected maximal X-ray energies. One of the important quality index of the radiographic system with the option of discrimination of TO material and their constituents is a precision of the discrimination parameters. This index is essentially dependent from many factors, for example, from the range of effective atomic numbers and from TO constituent sizes, from the given error of the discrimination parameter, from the maximal high energy of X-ray radiation. The state of the art analysis shows that the estimation task of the discrimination quality of the TO material and their constituents for major implementations of the discrimination method by dual high energy method is not solved in corpore.

2. The estimation of the discrimination parameter errors for the dual high energy method

To solve the problem of the discrimination TO materials and their constituents by DEM there are used different versions of two major approaches [8]. The first approach estimates the effective atomic number of the TO material. The second approach [8] generates the discrimination parameter image.



The value of every image point is compared with some level lines, and the comparison result is used to correlate T material with one or another class of material. The mentioned approaches are differed essentially by the volume of used preliminary information and by the algorithms of the primary radiograph processing therefore it is necessary to consider a specific character of the mathematical models to discriminate TO materials by use the DEM for the both abovementioned approaches.

Let consider some common part of the abovementioned discrimination approaches.

2.1. Common part

On the output of the digital radiographic system with the TO material discrimination option the maximal X-ray energies E_i , $i=1,2$ are corresponded to the primary radiographs $\mathbf{J}_i = \{J_i(x, y) : (x, y) \in S\}$, $i = 1,2$, where S is a discrete set of \mathbb{R}^2 . The physical meaning of the primary radiographs is the distribution of the absorbed energy of the primary attenuated X-ray radiation along the set S .

In the introduction we emphasized that the major characteristic of the discrimination quality is the discrimination parameters error, which evidently related with noise level of the primary radiographs. The research purpose of is to detect the mutual relation of the major customer characteristic with the cargo inspection system parameters, therefore we shall make more detailed analysis of the noise transformation during the step-by-step processing of the primary images.

On first stage we shall estimate the noise levels on the original images. In the first approximation we shall consider the radiation source as a point and isotropic one. Let suppose that the sensitivity volume of the singled radiometric detector has a rectangular prism form, which the center axis is oriented to the radiation source. The radiometric detector has size hd in the propagation direction of the primary X-ray beam, but in the perpendicular plane – $a_d \times b_d$. The distance between the radiation source and the front surface of the detector is equal to F . At the first stage of the design there is known some characteristic of the X-ray radiation source – P_{0max} , for example, the absorbed dose power or exposure dose of X-ray radiation on air at 1 meter distance and ν is a frequency of X-ray radiation impulses. The maximal energy E of X-ray radiation is adjustable value and can take values in the range from E_{min} to E_{max} . The control system of X-ray source can generate the sequence of alternated impulses with maximal energies E_1 and E_2 , $E_{min} < E_1 < E_2 < E_{max}$ according to a defined principle. We would name as an impulse package a collection of the serial X-ray radiation impulses, those need to produce a single line of the primary shadow radiographs J_1, J_2 , corresponding one another.

For the pulse X-ray radiation sources the time is measured in the pulse period – $1/\nu$. The number of impulses n in a package, which is need to generate a single line of the identification image, is equal to the sum of impulses with energy E_1 – n_1 and impulses with energy E_2 – n_2 . Here the identification image is a distribution of the calculated effective atomic number or discrimination parameter of the level lines method along the set S . The value n defines the inspection performance. The maximal performance of the radiographic system with option of the TO material discrimination and their constituents is reached for $n_1=1$, $n_2=1$. Evidently that in practice it is reasonable to advance a requirement $n_2 < n_1$. Let introduce a parameter $p=n_1/n_2$. If the parameter p and the number of impulses in the package n , are known that $n_2=n/(1+p)$ and $n_1=np/(1+p)$.

For the customer it is most interesting the minimal size of constituent, for which the material is surely discriminated by DEM. Let the projection of the specified constituent on the set S is consisted from M pixels.

Note that for every X-ray radiation source with the regulated maximal energy it is known a function W , which describes the dependence of the X-ray radiation source characteristic P_0 from the current value of the maximal energy E . Let the mentioned dependence has the following form

$$P_0(E) = P_{0max} W(E, E_{max}). \quad (1)$$

The function $W(E, E_{max})$ in the range of the maximal X-ray energies above 2 MeV is a smooth increasing function, for example, to describe the absorbed dose power [12] there is used the power dependence $W(E, E_{max})=(E/E_{max})^3$.

The number of photons N_{0i} of the X-ray radiation with the maximal energy E_i , whose are intersected the front surface of the single detector in the time unit when the test object is absent, is executed by formula

$$N_{0i} \approx \frac{CP_{0max} W(E_i, E_{max}) a_d b_d}{E_i \nu F^2 \int_0^{E_i} f(E, E_i) \mu_{ab\ air}(E) dE}, \quad (2)$$

where C is the conversion coefficient of the X-ray radiation source characteristic to dimension MeV/sec; $f(E, E_i)$ is the energy spectrum of the X-ray radiation with maximal energy E_i ; $\mu_{ab\ air}(E)$ is the linear absorption coefficient of the proton radiation with energy E in the air.

Let the X-ray radiation flow is weakened by the test object with the thickness ρH and the material's effective atomic number Z . In this case the number of photons $N_i(\rho H, Z)$ of the X-ray radiation with the maximal energy E_i , whose are not interacted with the TO and are registered by the radiometric detector in the time unit, is defined by the approximate expression

$$N_i(\rho H, Z) \approx N_{0i} \int_0^{E_i} f(E, E_i) e^{-m(E, Z) \rho H} [1 - e^{-\mu_d(E) h_d}] dE, \quad (3)$$

where $m(E, Z)$ is the mass attenuation coefficient of the photon radiation with energy E by the test object material; $\mu_d(E)$ is the linear attenuation coefficient of the proton radiation with energy E by the detector material.

The formula to estimate the radiometric signal beyond the test object thickness ρH and the effective atomic number Z is $I_i(\rho H, Z)$, $i=1,2$ without contribution of the background noises of the radiometric detectors has the form

$$I_i(\rho H, Z) = N_i(\rho H, Z) n_i \overline{E_{iab}(\rho H, Z)}, \quad (4)$$

where $\overline{E_{iab}(\rho H, Z)}$ is the mean value of the absorbed energy of the registered X-ray photon with maximal energy E_i beyond the testing object. The values $\overline{E_{iab}(\rho H, Z)}$ are calculated by the following way

$$\overline{E_{iab}(\rho H, Z)} = \frac{\int_0^{E_i} \overline{E_{ab}(E)} f(E, E_i) e^{-m(E, Z) \rho H} [1 - e^{-\mu(E) h_d}] dE}{\int_0^{E_i} f(E, E_i) e^{-m(E, Z) \rho H} [1 - e^{-\mu(E) h_d}] dE}, \quad (5)$$

where $\overline{E_{ab}(E)}$ is the mean energy value of the registered photon with energy E [13].

The dispersion of the radiometric signals $I_i(\rho H, Z) - DI_i(\rho H, Z)$, $i=1,2$ are calculated by formula [13]

$$DI_i(\rho H, Z) = n_i N_i(\rho H, Z) \overline{E_{iab}^2(\rho H, Z)} = n_i N_i(\rho H, Z) \overline{E_{iab}(\rho H, Z)}^2 \eta_i^2(\rho H, Z), \quad (6)$$

where $\overline{E_{iab}^2(\rho H, Z)}$ and $\eta_i^2(\rho H, Z)$ are the mean values of the absorbed energy square for the registered photons and the accumulation coefficient of fluctuations for X-ray radiation with the maximal energy E_i beyond the testing object under investigation. The formula to calculate $\overline{E_{iab}^2(\rho H, Z)}$ has the form similar to (5)

$$\overline{E_{ab}^2(\rho H, Z)} = \frac{\int_0^{E_i} \overline{E_{ab}^2(E)} f(E, E_i) e^{-m(E, Z) \rho H} [1 - e^{-\mu(E) h_d}] dE}{\int_0^{E_i} f(E, E_i) e^{-m(E, Z) \rho H} [1 - e^{-\mu(E) h_d}] dE}, \quad (7)$$

where $\overline{E_{ab}^2(E)}$ is the mean value of the energy square of the registered photon with energy E , which can be calculated, for example, by use formulas from [13].

After substitution (3) and (7) to formula (6) we get the expression coupling the dispersion $DI_i(\rho H, Z)$ with the number of impulses n_i .

$$DI_i(\rho H, Z) = N_i(\rho H, Z) n_i \frac{\int_0^{E_i} \overline{E_{ab}^2(E)} f(E, E_i) e^{-m(E, Z) \rho H} [1 - e^{-\mu(E) h_d}] dE}{\int_0^{E_i} f(E, E_i) e^{-m(E, Z) \rho H} [1 - e^{-\mu(E) h_d}] dE}. \quad (8)$$

At the next stage we consider the process of the noise transformation during the generation from primary images J_i the resulting radiographs $\mathbf{R}_i = \{R_i(x, y) : (x, y) \in S\}$.

The transformation of the primary images J_i to the resulting images R_i is consisted from several transformations, whose are the «black» calibration, the «white» calibration, the normalization on the reference detector signal, taking the logarithm. The «black» calibration is reduced to the subtraction of the mean values of the background noises levels of the radiometric detectors J_b . For the detectors J_b can be the determined values. During the «white» calibration the signals from the detectors are normalized on the signals without the testing object $I_{0i} = J_{0i} - J_b$ is the calibration. The transformation of the original radiometric signals $J_i(x, y)$ to $I_i(x, y)$, and then to $R_i(x, y)$ is described by formula

$$R_i(x, y) = -\ln \frac{J_i(x, y) - J_b}{J_{0i} - J_b} = -\ln \frac{I_i(x, y)}{I_{0i}}. \quad (9)$$

The values of $R_i(x, y)$ are numerically equal to the ray-lengths of the testing object for the X-ray radiation with the maximal energy E_i along the line, connecting the source point and the detector point with coordinates (x, y) , the measurement unit is the length of mean free path.

The dispersions R_1 and R_2 are estimated by use decomposition of (9) on small increments. The final expressions to calculate the dispersions $DR_1(\rho H, Z)$ and $DR_2(\rho H, Z)$ for the testing object thickness ρH and the effective atomic number Z have the form

$$DR_i(\rho H, Z) = \frac{DI_i(\rho H, Z)}{I_i^2(\rho H, Z)} + \frac{DI_i(0, 0)}{I_i^2(0, 0)}, \quad (10)$$

where $I_i(0, 0)$, $DI_i(0, 0)$ are the signal value and the signal dispersion when the testing object is absent. With including (4), (8) the expression (10) would have the following form

$$DR_i(\rho H, Z) = \frac{\tau_i(\rho H, Z)}{n_i}, \quad \tau_i(\rho H, Z) = \frac{\eta_i^2(\rho H, Z)}{N_i(\rho H, Z)} + \frac{\eta_i^2(0, 0)}{N_i(0, 0)}, \quad (11)$$

where $N_i(0, 0)$, $\eta_i(0, 0)$ are the number of protons registered by detector and the accumulation coefficient of fluctuations without the testing object.

Note 1. In practice the «white» calibration is carried out by the large number of the image lines k_0 , therefore the parameter estimations τ_i are defined by the expression

$$\tau_i(\rho H, Z) = \frac{\eta_i^2(\rho H, Z)}{N_i(\rho H, Z)} + \frac{\eta_i^2(0, 0)}{k_0 N_i(0, 0)}, \quad (12)$$

where $\overline{N_i(0,0)}$ is the selective mean of the photon number registered by detector without the testing object. For large values of k_0 the second summand in sums (11), (12) can be not included.

At the next stage the further transformations of the noise levels are depended from the image processing algorithms.

Note 2. The expressions to estimate the dispersions $R_1(\rho H, Z)$ and $R_2(\rho H, Z)$ for the testing object thickness ρH and the effective atomic number Z (10), (11) are derived without consideration of the pulsed X-ray radiation instability. In this case the instability means that the parameters characterized the single X-ray radiation pulse are the random values. The instability influence minimization is achieved by the normalization of the detector signals $I_i(\rho H, Z)$ on the signals from the reference detector I_{pi} . The reference detector signals I_{pi} are not dependent from the testing object. The expression to estimate the dispersion of the normalized signal $I_i(\rho H, Z)/I_{pi} - D(I_i(\rho H, Z)/I_{pi})$ has the following form

$$D\left(\frac{I_i(\rho H, Z)}{I_{pi}}\right) = \frac{I_{pi}^2 D I_i(\rho H, Z) + I_i^2(\rho H, Z) D I_{pi}}{I_{pi}^4}. \quad (13)$$

The expression (13) was derived for the condition of the full compensation of instability, which can be reached in that case when only the number of electrons dropped on the accelerator's target is instable [14].

From analysis of expression (13) it follows that during implementation of some requirements to the reference channel the estimation of the signal dispersions $R_1(\rho H, Z)$ and $R_2(\rho H, Z)$ can be done by the expressions (10), (12) whereas the first note. The abovementioned requirements in the formalized form look like

$$I_{pi} \gg I_i(\rho H, Z). \quad (14)$$

The physical implementation of the restriction (14) is reduced to use as the reference channel the special selected radiometric detector working synchronously with the measurement channels and distinguish from them by the large amount of registered photons and by the low value of the fluctuation accumulation coefficient.

2.2. Discrimination by the effective atomic number

As result of the combined processing of the resulting radiographs R_1 and R_2 there are producing the DEM parameters images – **A** and **B**. To estimate DEM parameters $A(x,y)$ and $B(x,y)$ for every point (x,y) of set S there is solved the non-linear equation system

$$\begin{aligned} -\ln \frac{\int_0^{E_1} \overline{E_{ab}(E)} f(E, E_1) e^{-A(x,y)w_1(E)-B(x,y)w_2(E)} [1 - e^{-\mu(E)h_d}] dE}{\int_0^{E_1} \overline{E_{ab}(E)} f(E, E_1) [1 - e^{-\mu(E)h_d}] dE} &= R_1(x, y) \\ -\ln \frac{\int_0^{E_2} \overline{E_{ab}(E)} f(E, E_2) e^{-A(x,y)w_1(E)-B(x,y)w_2(E)} [1 - e^{-\mu(E)h_d}] dE}{\int_0^{E_2} \overline{E_{ab}(E)} f(E, E_2) [1 - e^{-\mu(E)h_d}] dE} &= R_2(x, y), \end{aligned} \quad (15)$$

where $w_1(E)$, $w_2(E)$ are the energy dependencies of two main types of the photon radiation interaction with the testing object material. The first process in the system (15) is the Compton effect and the second one is the pair production.

To solve the system (15) relative to the parameters $A(x,y)$ and $B(x,y)$ it is necessary know the maximal energy values – E_1 and E_2 , the energy spectra $f(E, E_1)$ and $f(E, E_2)$, the energy dependencies $\overline{E_{ab}(E)}$, $w_1(E)$ and $w_2(E)$. There are known the analytical descriptions of the energy dependencies of

the mean value of the registered photon energy [13] and the interaction cross-section of the photon radiation with the material, for example [15]. Besides the analytical dependencies we can use the database of the gamma radiation interaction with the material [16, 17].

The certain complication during the organization of the preliminary information for the system (15) is related with the estimation of the energy spectra of the high-energy X-ray radiation. At the present time there is used the analytical approach to describe $f(E, E_i)$, which is based on the Schiff's formula [18–20] adjusted for the attenuation in the radiation source filters and adjusted for the registration efficiency of the photon radiation.

During solution of the system (15) the random value dispersions A , B – DA and DB , and also the covariation $cov(A, B)$ are founded by the least increments method application. The final expressions for the dispersions $DA(\rho H, Z)$, $DB(\rho H, Z)$ and the covariation $cov(A, B)(\rho H, Z)$ for the testing object thickness ρH and the effective atomic number Z have the form

$$\begin{aligned} DA(\rho H, Z) &= \frac{g_{22}^2 DR_1(\rho H, Z) + g_{12}^2 DR_2(\rho H, Z)}{G^2(\rho H, Z)}, \\ DB(\rho H, Z) &= \frac{g_{11}^2 DR_2(\rho H, Z) + g_{21}^2 DR_1(\rho H, Z)}{G^2(\rho H, Z)}, \\ cov(A, B)(\rho H, Z) &= \frac{-g_{22}g_{21}DR_1(\rho H, Z) - g_{12}g_{11}DR_2(\rho H, Z)}{G^2(\rho H, Z)}. \end{aligned} \quad (16)$$

where

$$\begin{aligned} g_{ij} &= g_{ij}(\rho H, Z) = \frac{\int_0^{E_i} w_j(E) \overline{E_{ab}(E)} f(E, E_1) e^{-m(E, Z)\rho H} [1 - e^{-\mu(E)h_d}] dE}{\int_0^{E_i} \overline{E_{ab}(E)} f(E, E_1) e^{-m(E, Z)\rho H} [1 - e^{-\mu(E)h_d}] dE}, \\ G(\rho H, Z) &= g_{11}(\rho H, Z)g_{22}(\rho H, Z) - g_{12}(\rho H, Z)g_{21}(\rho H, Z). \end{aligned}$$

The substitution (11) in (16) gives

$$\begin{aligned} DA(\rho H, Z) &= \frac{g_{22}^2 \tau_1(\rho H, Z)/n_1 + g_{12}^2 \tau_2(\rho H, Z)/n_2}{G^2(\rho H, Z)}, \\ DB(\rho H, Z) &= \frac{g_{11}^2 \tau_2(\rho H, Z)/n_2 + g_{21}^2 \tau_1(\rho H, Z)/n_1}{G^2(\rho H, Z)}, \\ cov(A, B)(\rho H, Z) &= \frac{-g_{22}g_{21} \tau_1(\rho H, Z)/n_1 - g_{12}g_{11} \tau_2(\rho H, Z)/n_2}{G^2(\rho H, Z)}. \end{aligned} \quad (17)$$

The final research stage of the noise transformation is connected with the estimation of the effective atomic number dispersion. In the high-energy domain [8] the effective atomic number estimation $Z_V(\rho H, Z)$ is related to the DEM parameters by the following expressions $A(\rho H, Z)$ and $B(\rho H, Z)$ [8]

$$Z_V(\rho H, Z) \approx \frac{B(\rho H, Z)}{A(\rho H, Z)}. \quad (18)$$

Applying the least increments method to (18) we get for the testing object thickness ρH and the material's effective atomic number – Z the formula to calculate the dispersion of the effective atomic number estimation $Z_V(\rho H, Z) - DZ_V(\rho H, Z)$

$$DZ_V(\rho H, Z) \approx \frac{A^2 DB(\rho H, Z) + B^2 DA(\rho H, Z) - 2AB cov(A, B)(\rho H, Z)}{A^4}. \quad (19)$$

Let substitute the expression (17) in the formula (19). After simple conversions the expression to estimate the effective atomic number dispersion reduce to the form

$$DZ_v(\rho H, Z) \approx \frac{(Ag_{21} + Bg_{22})^2 \tau_1(\rho H, Z)/n_1 + (Ag_{11} + Bg_{12})^2 \tau_2(\rho H, Z)/n_2}{G^2(\rho H, Z)A^4}. \quad (20)$$

We are interesting in the relation of the dispersion of the estimated testing object parameter $DZ_v(\rho H, Z)$ with the number of pulses in the package $n=n_1+n_2$, with the parameter $p= n_1/n_2$ and with the physical TO characteristics – the mean value of the material's effective atomic number Z and with the thickness ρH . The parameters of the high-energy implementation of DEM $A(\rho H, Z)$ and $B(\rho H, Z)$ are related to Z and ρH by the following way [8]

$$A(\rho H, Z) = \rho H, \quad B(\rho H, Z) = Z\rho H. \quad (21)$$

After substitution of (21) in (20) under conditions $n_2=n/(1+p)$ and $n_1=np/(1+p)$ we get

$$DZ_v(\rho H, Z) \approx \frac{(1+p)[(g_{21} + Zg_{22})^2 \tau_1(\rho H, Z)/p + (g_{11} + Zg_{12})^2 \tau_2(\rho H, Z)]}{nG^2(\rho H, Z)(\rho H)^2}. \quad (22)$$

The expression (22) together with formulas (11), (12) allow to estimate the measurement accuracy of the TO material's effective atomic number, in term of the time to generate lines of the primary radiographs, the TO parameters, the maximal energies of the X-ray radiation. The measurement accuracy of the effective atomic number Z can be estimated by the least-square deviation ΔZ – $\Delta Z_v(\rho H, Z) = \sqrt{DZ_v(\rho H, Z)}$.

Evidently, that there is exist the optimal value of the parameter p , for which the dispersion value $DZ_v(\rho H, Z)$ under fixed values Z and ρH is minimal. The formula to calculate p_{opt} has form

$$p_{opt}(\rho H, Z) = \frac{g_{21} + Zg_{22}}{g_{11} + Zg_{12}} \sqrt{\frac{\tau_1(\rho H, Z)}{\tau_2(\rho H, Z)}}. \quad (23)$$

The dispersion value $DZ_v(\rho H, Z)$ corresponding to p_{opt} , is defined by substitution (23) in (22).

The formula (22) can calculate the number of pulses in the package which need to generate the line's pair of the images I_1 and I_2 , on the basis of the user defined maximal deviation of the effective atomic number ΔZ_{lim} . The mentioned maximal deviation of the effective atomic number ΔZ_{lim} is named the resolution by Z . The unknown expression has the form

$$n(\rho H, Z) \approx \frac{(1+p)[(g_{21} + Zg_{22})^2 \tau_1(\rho H, Z)/p + (g_{11} + Zg_{12})^2 \tau_2(\rho H, Z)]}{G^2(\rho H, Z)(\rho H)^2 \Delta Z_{lim}^2}. \quad (24)$$

Note 3. The expressions (20)–(22), (24) were derived for the case when the estimation of the effective atomic number of the testing object material or their constituent $Z_v(\rho H, Z)$ are produced for one identification image point (one pixel). In practice the image of the minimal constituent defined by user consist of M pixels $M \gg 1$. Therefore it is logically to use the mean estimation value of the effective atomic number $\overline{Z_v(\rho H, Z)}$ as the identification parameter. The dispersion of mean value $\overline{DZ_v(\rho H, Z)}$ is defined by the formula

$$\overline{DZ_v(\rho H, Z)} = \frac{DZ_v(\rho H, Z)}{M}. \quad (25)$$

Including (25) the all mentioned in Note 3 the formulas are corrected by including the additional factor equal to $1/M$ into the right part.

Note 4. The inspection efficiency is essentially depended of the testing object thickness ρH . The internal structure randomness of the inspecting objects creates some dilemma before the customer.

This dilemma must give the answer to the question – what is more preferable – the high inspection efficiency with the qualified discrimination of the testing object materials and their constituents with small thickness or the low inspection efficiency with the qualified discrimination of the large thickness material.

2.3. Discrimination by the level lines method

The second implementation of the testing object discrimination and their constituents by DEM we named the level lines method [8]. In this implementation on the base of resulting images R_1 and R_2 the identification image is created

$$\mathbf{Q} = \left\{ Q(x, y) = \frac{R_2(x, y)}{R_1(x, y)} : (x, y) \in S \right\}. \quad (26)$$

The testing object material in the point with coordinates (x, y) is correlated with some material, if the following restriction is carried out

$$U_-(R_1(x, y)) < Q(R_1(x, y)) \leq U_+(R_1(x, y)), \quad (27)$$

where $U_-(x, y)$, $U_+(x, y)$ are the level lines for the correlated material.

For the testing object thickness ρH and the material's effective atomic number Z the identification parameter dispersion $Q(\rho H, Z) - DQ(\rho H, Z)$ is defined by the small increment decomposition

$$DQ(\rho H, Z) = \frac{R_1^2(\rho H, Z)DR_2(\rho H, Z) + R_2^2(\rho H, Z)DR_1(\rho H, Z)}{R_1^4(\rho H, Z)}. \quad (28)$$

After substitution (10), (11) in (28) including $n_2 = n/(1+p)$ and $n_1 = np/(1+p)$ we get

$$DQ(\rho H, Z) = \frac{(1+p)[R_1^2(\rho H, Z)\tau_2(\rho H, Z) + R_2^2(\rho H, Z)\tau_1(\rho H, Z)/p]}{nR_1^4(\rho H, Z)}. \quad (29)$$

The collection of the expressions (3), (9), (11) and (29) allows to estimate the identification parameter accuracy by the level lines method – $\Delta Q(\rho H, Z) = \sqrt{DQ(\rho H, Z)}$.

The value of the parameter $p - p_{\text{opt}}(\rho H, Z)$, for which the value $DQ(\rho H, Z)$ is minimal, is calculated by the formula

$$p_{\text{opt}}(\rho H, Z) = \frac{R_2(\rho H, Z)}{R_1(\rho H, Z)} \sqrt{\frac{\tau_1(\rho H, Z)}{\tau_2(\rho H, Z)}}. \quad (30)$$

The minimal dispersion value $DQ(\rho H, Z)$ is defined by substitution (30) in the expression (29).

The total number of pulses n , which determine the cargo inspection performance with the material discrimination by the level lines method, is calculated from (29), starting from the limiting accuracy of the identification parameter ΔQ_{lim} ,

$$n(\rho H, Z) = \frac{(1+p)[R_1^2(\rho H, Z)\tau_2(\rho H, Z) + R_2^2(\rho H, Z)\tau_1(\rho H, Z)/p]}{R_1^4(\rho H, Z)\Delta Q_{\text{lim}}^2}. \quad (31)$$

The expressions (3), (9), (11), (31) allow to estimate the cargo inspection performance with the option of the material discrimination by level lines method. The notes 3 and 4 from the previous section must take into account.

3. Calculation ΔZ_V and ΔQ

To show the applicability of the above mentioned algorithms for estimation of the identification parameter accuracy by high-energy DEM there was carried out the series of the mean-square deviation calculation for the identification parameter for two pairs of the maximal values of the X-ray radiation

– $E_1=4.5$ MeV, $E_2=7.5$ MeV and $E_1=4.5$ MeV, $E_2=9$ MeV. The testing object thickness ρH was varied from 10 to 120 g/cm², but the effective atomic number Z take the values 6, 13, 26 and 82. The calculations were done for betatron MIB-4/9 with characteristics $P_{0max}=20$ R/min for and $E_{max}=9$ MeV, $\nu=200$ pulses per second. The inspection geometry was characterized by the parameters: the focal length $F=4.2$ m; the radiometric detectors on base of the CdWO₄ scintillator with thickness $h_d=50$ mm and the lateral sizes $a_d \times b_d = 5 \times 6$ mm². The values $n_1=3$, $n_2=1$. The minimal number of pixels in the projection on the mapping surface for the surely identified constituent is $M=16$.

The tables 1 and 2 show the calculation results ΔZ_V and ΔQ for the different thicknesses ρH and the different testing object materials.

Table 1. The dependence of the mean-square deviation for the effective atomic number ΔZ_V from ρH .

Material	$E_1 - E_2$, MeV	ρH , g/cm ²											
		10	20	30	40	50	60	70	80	90	100	110	120
C	4.5 – 7.5	11.2	6.6	5.1	4.5	4.2	4.2	4.2	4.3	4.5	4.7	5.0	5.4
	4.5 – 9	5.6	3.3	2.6	2.3	2.2	2.1	2.2	2.2	2.3	2.5	2.6	2.8
Al	4.5 – 7.5	11.4	6.8	5.3	4.7	4.5	4.4	4.5	4.6	4.8	5.1	5.5	5.9
	4.5 – 9	5.8	3.4	2.7	2.5	2.3	2.3	2.4	2.4	2.6	2.7	2.9	3.2
Fe	4.5 – 7.5	12.0	7.2	5.8	5.3	5.1	5.1	5.2	5.4	5.8	6.2	6.8	7.4
	4.5 – 9	6.1	3.8	3.1	2.8	2.7	2.7	2.8	3.0	3.2	3.5	3.8	4.2
Pb	4.5 – 7.5	14.6	9.5	8.3	8.0	8.0	8.6	9.3	10.3	11.6	13.2	15.1	17.5
	4.5 – 9	8.0	5.3	4.7	4.6	4.7	5.1	5.5	6.2	7.0	8.1	9.3	10.8

The analysis of the data mentioned in the table 1, shows that the accuracy of Z is high for the small and large thicknesses. The accuracy of Z is reduced with increasing of the greater energy.

Table 2. The dependence of the mean-square deviation of the discrimination parameter $\Delta Q \times 0.01$ from ρH .

Material	$E_1 - E_2$, MeV	ρH , g/cm ²											
		10	20	30	40	50	60	70	80	90	100	110	120
C	4.5 – 7.5	1.10	0.81	0.75	0.76	0.79	0.85	0.92	1.01	1.12	1.24	1.39	1.56
	4.5 – 9	0.94	0.69	0.64	0.64	0.66	0.71	0.77	0.85	0.94	1.05	1.17	1.32
Al	4.5 – 7.5	1.10	0.82	0.76	0.77	0.80	0.86	0.93	1.02	1.13	1.26	1.41	1.58
	4.5 – 9	0.94	0.67	0.65	0.65	0.68	0.73	0.79	0.87	0.96	1.07	1.21	1.36
Fe	4.5 – 7.5	1.08	0.83	0.77	0.78	0.82	0.88	0.96	1.06	1.18	1.32	1.49	1.68
	4.5 – 9	0.93	0.71	0.66	0.67	0.70	0.76	0.83	0.92	1.02	1.15	1.30	1.47
Pb	4.5 – 7.5	0.25	0.29	0.33	0.39	0.46	0.54	0.63	0.75	0.89	1.06	1.27	1.51
	4.5 – 9	0.23	0.26	0.30	0.36	0.42	0.49	0.58	0.69	0.82	0.98	1.16	1.39

The analysis of the data mentioned in the table 2 shows that the accuracy of the identification parameter Q has less evident dependence from ρH and the larger maximal energy, than the accuracy of Z .

4. Experiments

To verification the efficiency of algorithms designed to estimate the material identification parameter accuracy by use different implementation of the DEM, there was done the series of the experiments on the cargo inspection system of the Tomsk polytechnic university. The testing object composed from the constituents with different thicknesses from the organic materials, aluminum, iron and lead, was scanned by two narrow X-ray beams $E_1=4.5$ MeV, $E_2=9$ MeV. The experimental conditions were differed from the calculation conditions only by the power of the exposition dose – $P_{0max}=5$ R/min. The indicated power was selected to provide the stable work of the betatron for a long time. The figures 1 and 2 show the results of the comparison the experimental and the numerical dependencies $\Delta Z_V(\rho H)$ and $\Delta Q(\rho H)$.

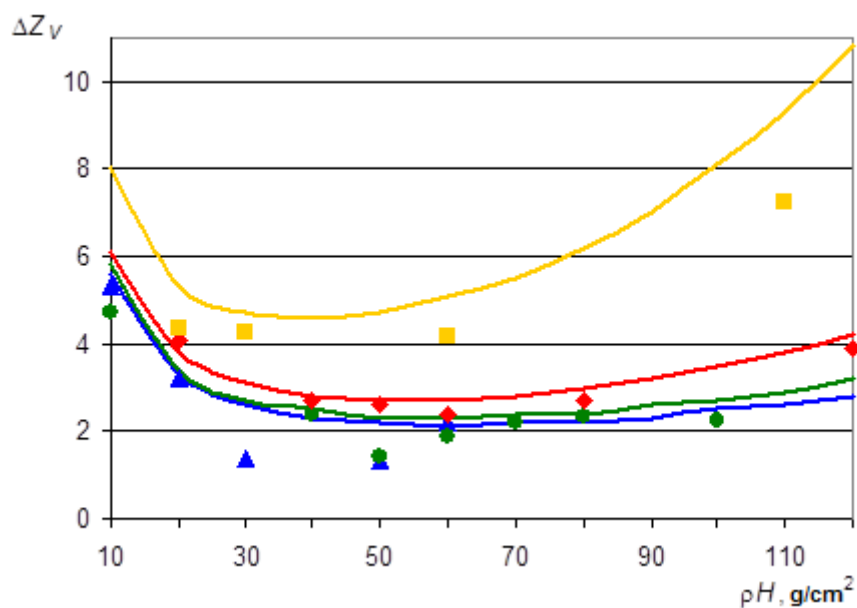


Figure 1. The calculated and the experimental dependencies $\Delta Z_V(\rho H)$:

- calculation, ■ — experiment, material – Pb;
- calculation, ◆ — experiment, material – Fe;
- calculation, ● — experiment, material – Al;
- calculation, ▲ — experiment, organics.

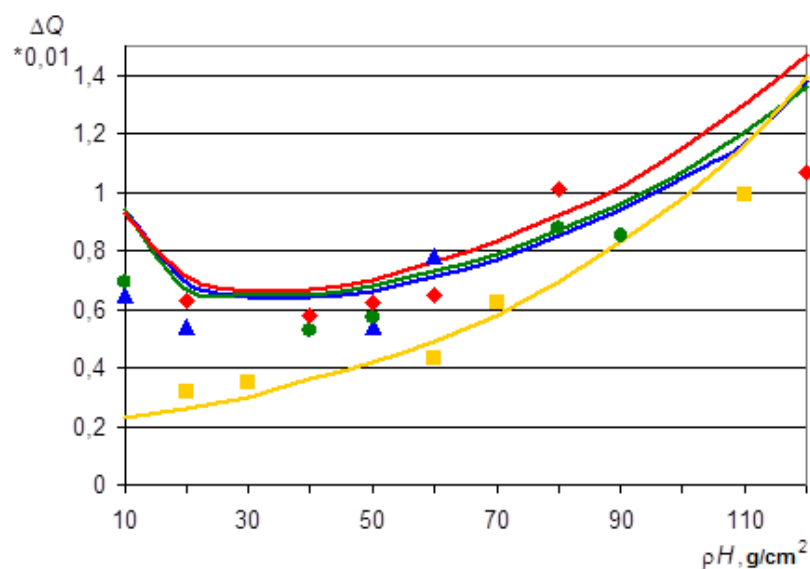


Figure 2. The calculated and the experimental dependencies $\Delta Q(\rho H)$:

- calculation, ■ — experiment, material – Pb;
- calculation, ◆ — experiment, material – Fe;
- calculation, ● — experiment, material – Al;
- calculation, ▲ — experiment, organics.

From analysis of the data presented on figures 1 and 2 it follows that in the considered range of the test object thicknesses the experimental estimations of the identification DEM parameter accuracy are closes to the numerical ones, or less than ones. It proves the applicability of the proposed algorithms to estimate accuracy of the effective atomic number and the identification parameter of the level lines method in practice.

5. Relation between impulses in the package

In section 2 it was shown that the DEM identification parameters accuracy is essentially depending from value p . The parameter p is equal to the ratio of the number of the pulses with the less maximal X-ray energy in the package to the one with the larger maximal energy. Before it was emphasized that there are exist the optimal values of the parameter $p - p_{opt}$, for which the dispersion values of the identification parameters are minimal.

The parameter p_{opt} for the identification parameter Z is calculated by use the formula (23), and for the identification parameter Q – with use the expression (30). The series of the calculation of the dependencies $p_{opt}(\rho H, Z)$ for the identification parameters Z and Q for the conditions of the numerical example from section 3 was carried out. The dependencies $p_{opt}(\rho H)$ for the objects from carbon, aluminum, iron and lead are given in the table 3.

From analysis of the data in the table 3 a number of conclusions can be done. The first conclusion – with increasing the object thickness ρH the values p_{opt} are increased during identification by Q and by Z . The second conclusion – the values p_{opt} for the Q identification are practically closed to the similar values p_{opt} , for the Z identification the divergence is not more than 10 %. The third conclusion – the values p_{opt} for the usage of the pair of maximal energies 4.5 – 9 MeV are always large than values p_{opt} for the usage of the maximal energies pair 4.5 – 7.5 MeV. We can make the following recommendations how to use the table 3. The number of pulses in the package n is selected by the formulas (24) or (31) including the notes 3, 4. The number of pulses of the larger energy n_2 is the maximum from two numbers – the nearest integer to $n/(1+p_{opt})$ and 1, but it is logically to get as n_1 the maximum of the nearest integer to $np_{opt}/(1+p_{opt})$ and 1.

Table 3. The optimal values p_{opt} .

Material	$E_1 - E_2$, MeV	ρH , g/cm ²												
		10	20	30	40	50	60	70	80	90	100	110	120	
C	Q	4.5 – 7.5	1.31	1.42	1.52	1.61	1.71	1.8	1.89	1.98	2.07	2.16	2.26	2.36
		4.5 – 9	1.45	1.61	1.76	1.9	2.05	2.19	2.34	2.49	2.64	2.79	2.95	3.12
	Z	4.5 – 7.5	1.31	1.41	1.52	1.61	1.71	1.8	1.89	1.99	2.08	2.17	2.27	2.36
		4.5 – 9	1.45	1.61	1.76	1.91	2.06	2.21	2.36	2.51	2.67	2.82	2.99	3.15
Al	Q	4.5 – 7.5	1.33	1.43	1.53	1.62	1.71	1.79	1.87	1.95	2.03	2.11	2.19	2.27
		4.5 – 9	1.47	1.63	1.78	1.92	2.05	2.19	2.32	2.45	2.58	2.71	2.84	2.98
	Z	4.5 – 7.5	1.34	1.44	1.54	1.63	1.71	1.8	1.88	1.97	2.05	2.13	2.21	2.29
		4.5 – 9	1.5	1.65	1.8	1.95	2.09	2.23	2.36	2.5	2.64	2.77	2.91	3.05
Fe	Q	4.5 – 7.5	1.35	1.47	1.56	1.64	1.72	1.79	1.86	1.93	2	2.06	2.12	2.18
		4.5 – 9	1.51	1.69	1.83	1.96	2.08	2.2	2.31	2.42	2.52	2.62	2.73	2.83
	Z	4.5 – 7.5	1.4	1.5	1.59	1.67	1.74	1.82	1.89	1.96	2.03	2.09	2.15	2.22
		4.5 – 9	1.6	1.76	1.9	2.03	2.15	2.28	2.39	2.5	2.62	2.72	2.83	2.94
Pb	Q	4.5 – 7.5	1.84	1.9	1.95	1.99	2.02	2.06	2.08	2.11	2.14	2.16	2.18	2.21
		4.5 – 9	2.3	2.38	2.45	2.52	2.57	2.62	2.66	2.7	2.74	2.78	2.81	2.85
	Z	4.5 – 7.5	1.68	1.8	1.88	1.94	2.00	2.05	2.09	2.13	2.16	2.2	2.23	2.25
		4.5 – 9	2.09	2.28	2.42	2.52	2.61	2.68	2.75	2.81	2.87	2.92	2.96	3.00

6. Results

There are given the collections of the mathematical relations whose allow to estimate the identification parameter accuracy for the two DEM implementations – the discrimination by the effective atomic number and the discrimination by the level lines method. The example of the identification parameter

accuracy calculation was done for the cargo inspection system of the Tomsk polytechnic university on the base of the portable betatron MIB-4/9. The results of the comparison the theoretical and the experimental estimations of the identification parameters accuracy proved the applicability of the proposed algorithms to validate the quality of the radiographic systems with the material discrimination option for the testing object and their constituents. There are formulated the recommendations to select a structure of the package of X-ray radiation impulses, which produce a single line of the dual energy image.

7. Acknowledgement

The authors are very much obliged to the support of the Russian Foundation for Basic Research (grant 13-08-98027), National research Tomsk polytechnic university (grant VIU INK 66 2014) and the company PowerScan Technologies Ltd (Beijing, China).

References

- [1] Kolkoori S, Wrobel N, Osterloh K, Redmer B, Deresch A and Ewert U 2013 High-energy radiography for detecting details in highly complex packings *MP Mater Test.* **55** 683–8
- [2] Mery D 2014 Computer vision technology for X-ray testing *Insight-non-destructive testing and condition monitoring.* **56** 147–55
- [3] Martins M N and Silva T F 2014 Electron accelerators: History, applications, and perspectives *Radiat Phys Chem.* **95** 78–85
- [4] Ryzhikov V D, Opolonin O D, Lysetska O K, Galkin S M, Voronkin Y F and Perevertaylo V L 2013 Research on improvement of receiving-detecting circuit for digital radiographic systems with advanced spatial resolution *Nondestructive testing of materials and structures. Springer Netherlands* **6** 105–9
- [5] Wells K and Bradley D A 2012 A review of X-ray explosives detection techniques for checked baggage *Appl Radiat Isotopes* **70** 1729–46
- [6] Rebuffel V and Dinten J M 2007 Dual-energy X-ray imaging: benefits and limits *Insight-non-destructive testing and condition monitoring* **49** 589–94
- [7] Beldjoudi G, Rebuffel V, Verger L, Kaftandjian V and Rinkel J 2012 An optimised method for material identification using a photon counting detector *Nucl Instrum Meth A* **663** 26–36
- [8] Chakhlov S V and Osipov S P 2013 High-energy digital X-ray imaging method for substance identification *Kontrol'. Diagnostika* **9** 9–17
- [9] Ji Sung, Park and Jong Kyung Kim 2011 Calculation of effective atomic number and normal density using a source weighting method in a dual energy X-ray inspection system *J Korean Phys Soc.* **59** 2709–13
- [10] Klimenov V A, Osipov S P and Temnik A K 2013 Identification of the substance of a test object using the dual-energy method *Russian J Nondestr Test.* **49** 642–9
- [11] Osipov S P, Temnik A K and Chakhlov S V 2014 The effects of physical factors on the quality of the dual high energy identification of the material of an inspected object *Russian J Nondestr Test.* **50** 491–8
- [12] Ananiev L M and Stein M M 1971 On the question of the mathematical description of the betatron *Bulletin of the Tomsk Polytechnic Institute* **180** 3–7
- [13] Zav'yalkin, F.M. and Osipov, S.P. 1985 Dependence of the mean value and fluctuations of the absorbed energy on the scintillator dimensions *At Energ.* **59** 281–3
- [14] Zav'yalkin F M and Osipov S P 1989 Effect of the instability of parameters of bremsstrahlung beams on the accuracy of radiometric measurements *Sov J Nondestr Test.* **25** 108–12
- [15] Siegbahn K 2012 *Alpha-, beta-and gamma-ray spectroscopy* (Burlington, MA : Elsevier)
- [16] Gamma data for elements. <http://www.ippe.ru/podr/abbn/libr/groupkon.php>
- [17] Chadwick M B, Obložinský P, Herman M, Greene N M, McKnight R D, Smith D L, Young P G, MacFarlane R E, Hale G M, Frankl S C, Kahler A C, Kawano T, Little R C, Madland D G, Moller P, Mosteller R D, Page P R, Talou P, Trellue H, White M C, Wilson W B, Arcilla R,

- Dunford C L, Mughabghab S F, Pritychenko B, Rochman D, Sonzogni A A, Lubitz C R, Trumbull T H, Weinman J P, Brown D A, Cullen D E, Heinrichs D P, McNabb D P, Derrien H, Dunn M E, Larson N M, Leal L C, Carlson A D, Block R C, Briggs J B, Cheng E T, Huria H C, Zerkle M L, Kozier K S, Courcelle A, Pronyaev V and Van der Marck S C 2006 ENDF/B-VII. 0: Next generation evaluated nuclear data library for nuclear science and technology *Nucl Data sheets* **107** 2931–3060
- [18] Schiff L I 1951 Energy-angle distribution of thin target bremsstrahlung *Phys Rev.* **83** 252–3
- [19] Aliev F K, Alimov G R, Muminov A T, Osmanov B S and Skvortsov V V 2005 Simulation of experiment on total external reflection of electron bremsstrahlung *Tech Phys.* **50** 1053–7.
- [20] Mordasov N G, Ivashchenko D M, Chlenov A M and Astakhov A A 2004 Simulation of methods for a rapid determination of the energy spectrum of bremsstrahlung from electron accelerators *Tech Phys.* **49** 1213–20